Journal of Power Sources 300 (2015) 77–86

Contents lists available at ScienceDirect

Journal of Power Sources

journal homepage: www.elsevier.com/locate/jpowsour

Electrochemical performance and capacity degradation mechanism of single-phase La–Mg–Ni-based hydrogen storage alloys

Jingjing Liu [a, b], Yuan Li [a, b], Da Han [c], Shuqin Yang [a, b], Xiaocui Chen [a, b], Lu Zhang [a, b], Shumin Han [a, b, *]

[a] State Key Laboratory of Metastable Materials Science and Technology, Yanshan University, Qinhuangdao 066004, PR China
[b] College of Environmental and Chemical Engineering, Yanshan University, Qinhuangdao 066004, PR China
[c] Department of Chemistry and Department of Physiology and Function Genomics, Center for Research at the Bio/Nano Interface, Shands Cancer Center and UF Genetics Institute, University of Florida, Gainesville, FL 32611-7200, United States

HIGHLIGHTS

- Single-phase AB_3-, A_2B_7- and A_5B_{19}-type La–Mg–Ni-based alloys are obtained.
- Relationship between subunit structure and electrochemical properties is studied.
- Behavior of [$LaNi_5$] and [$LaMgNi_4$] subunits during charge/discharge is observed.
- Mismatch between [$LaNi_5$] and [$LaMgNi_4$] is a basic cause for capacity degradation.

GRAPHICAL ABSTRACT

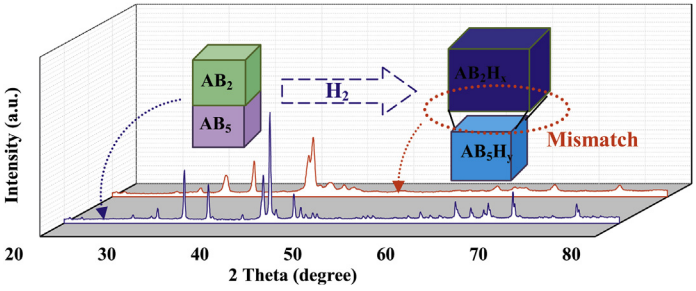

ARTICLE INFO

Article history:
Received 31 July 2015
Received in revised form
14 September 2015
Accepted 15 September 2015
Available online 24 September 2015

Keywords:
Metal hydride electrode
Single phase
Subunit structure
Electrochemical property
Cycling stability

ABSTRACT

La–Mg–Ni-based hydrogen storage alloys are a promising candidate for the negative electrode materials of nickel metal hydride batteries. However, their fast capacity degradation hinders them from more extensive application. In this study, the electrochemical performance and capacity degradation mechanism of single-phase La_2MgNi_9, La_3MgNi_{14} and La_4MgNi_{19} alloys are studied from the perspective of their constituent subunits. It is found that the rate capability and cycling stability of the alloy electrodes increase with higher [$LaNi_5$]/[$LaMgNi_4$] subunit ratio, while the discharge capacity shows a reverse trend. Degradation study shows that the inter-molecular strains in the alloys are the main reason that leads to the fast capacity degradation of La–Mg–Ni-based alloys. The strains are caused by the difference in the expansion/contraction properties between [$LaNi_5$] and [$LaMgNi_4$] subunits during charge/discharge which is mainly observed in the H-dissolved solid solution instead of hydride. It is also found that the strains can be relieved by adjusting [$LaNi_5$]/[$LaMgNi_4$] subunit ratio of the alloys, thus achieving less pulverization and oxidation, and better cycling stability. We expect our findings can inspire new thoughts on improving the electrochemical performance of La–Mg–Ni-based alloys by tuning their superlattice structures.

1. Introduction

Rare earth (RE)–Mg–Ni-based metal hydride (MH) alloys are one of the latest active materials applied for the negative electrodes

* Corresponding author. College of Environmental and Chemical Engineering, Yanshan University, Qinhuangdao 066004, PR China.
E-mail address: hanshm@ysu.edu.cn (S. Han).

http://dx.doi.org/10.1016/j.jpowsour.2015.09.058
0378-7753/

of nickel/metal hydride (Ni/MH) batteries [1]. This alloy system exhibits promising electrochemical properties, including large discharge capacity, easy activation and good high rate dischargeability (*HRD*). The discharge capacity of the La–Mg–Ni-based $La_5Mg_2Ni_{23}$ alloy could reach as high as 410 mAh g^{-1}, 25% higher than that of AB_5-type alloys [2,3]. However, their fast capacity degradation in alkaline electrolyte has been hindering them from wide application [3–5].

The fast electrochemical capacity degradation of La–Mg–Ni-based alloy electrodes is mainly attributed to pulverization and oxidation/corrosion. It has been reported that their degradation process could be divided into three sequential stages: 1) pulverization and Mg oxidation stage, 2) Mg and La oxidation stage and 3) oxidation-passivation stage [6]. Pulverization occurs at the initial stage of battery cycling, which increases the contact resistance between the alloy particles and decreases the charging/discharging efficiency. Moreover, smaller particles produced by pulverization are highly active in alkaline solution and are more sensitive to oxidation/corrosion [7,8]. Compared to AB_5-type hydrogen storage alloys, La–Mg–Ni-based hydrogen storage alloys suffer more drastic pulverization during cycling [7,9]. It was reported that the average particle size of La–Mg–Ni-based alloys dropped to 26.0 μm from 56.5 μm after only 40 charge/discharge cycles [8], whereas the average particle size of $LaNi_5$-type alloys was 23 μm even after 300 cycles [9]. These observations lead to the question of what factor caused such violent pulverization for La–Mg–Ni-based alloys during hydrogen absorption/desorption.

Unlike AB_5- or AB_2-type hydrogen storage alloys, La–Mg–Ni-based alloys are derived from La–Ni-based binary alloys consisting of $[AB_5]$ and $[A_2B_4]$ subunits stacking along *c* axis. For binary La–Ni-based alloy hydrides, hydrogen atoms are located only in $[A_2B_4]$ subunits and at the boundary between $[A_2B_4]$ and $[AB_5]$ subunits. This uneven distribution of hydrogen atoms is due to much bigger volume size of $[A_2B_4]$ subunits [10,11]. Thus, a significant volume expansion of the $[A_2B_4]$ subunits is introduced, while only a little expansion occurs in the $[AB_5]$ subunits, resulting in an expansion mismatch between $[A_2B_4]$ and $[AB_5]$ subunits. This mismatch causes serious strains in the alloys, which leads to pulverization/amorphization of alloy particles [12]. For ternary La–Mg–Ni-based alloys, although Mg substitution at the La site largely decreases the volume difference between $[A_2B_4]$ and $[AB_5]$ subunits and enables $[AB_5]$ subunits to absorb hydrogen, significant strains still exist during hydrogen absorption/desorption. Unexpectedly, the most significant strains do not occur at the full hydride stage where the cell volume expansion rate is the highest, but at the medium stage [10]. Therefore, understanding the cause of the generation and the varying trend of the internal strains in La–Mg–Ni-based alloys during the entire hydrogen absorption/desorption process is essential to recognize their cycling degradation mechanism and to further improve their cycling stability.

$(La,Mg)Ni_3$, $(La,Mg)_2Ni_7$ and $(La,Mg)_5Ni_{19}$ phases are the most common phases in La–Mg–Ni-based alloys. These three phases exhibit similar superstacking structures. The basic structural difference between these phases is the ratios of the intergrowing $[AB_5]$ and $[A_2B_4]$ subunits in their long-range stacking arrangement. The difference in the ratio and the neighboring environment of $[AB_5]$ and $[A_2B_4]$ constituent subunits is likely to be the root cause that leads to the variations in the overall hydrogen absorption/desorption behaviors as well as the electrochemical performance of these phases. In this study, single-phase La_2MgNi_9, La_3MgNi_{14} and La_4MgNi_{19} alloys with $[LaNi_5]/[LaMgNi_4]$ subunit ratios of 1:1, 2:1 and 3:1, respectively have been prepared, and the hydrogen absorption/desorption behaviors and electrochemical performance of the alloys are investigated in terms of the structural characteristics of their constituent subunits. Particularly, the degradation mechanism of the single-phase superlattice alloys is studied and the cause of the capacity degradation is identified. This study offers a fundamental understanding for improving the cycling stability of La–Mg–Ni-based alloys applied as the negative electrode materials for Ni/MH batteries.

2. Experimental

The La_2MgNi_9, La_3MgNi_{14} and La_4MgNi_{19} alloys were synthesized by step-wise sintering $LaMgNi_4$ and $LaNi_5$ precursor powders. The precursors were prepared by inductive melting La, Mg and Ni with purity higher than 99.5% under argon atmosphere, followed by annealing at 700 °C and 1000 °C for $LaMgNi_4$ and $LaNi_5$, respectively to guarantee their composition homogeneity. The precursors exhibited singe-phase structures as seen from the Rietveld refinements in Fig. S1. To prepare the target alloys, the $LaMgNi_4$ and $LaNi_5$ precursors were first ground into powders (<300 mesh) and mixed in molar ratios of 1:1, 1:2 and 1:3 for La_2MgNi_9, La_3MgNi_{14} and La_4MgNi_{19} alloys, respectively. Extra amount of Mg powder was added to the mixtures to compensate for Mg loss during the sintering process. The mixtures were first ball milled for an hour and then cold pressed into pellets. Each of the pellets was then wrapped into Ta foil and sealed in a nickel shell for sintering, as shown in the inset of Fig. 1. The sintering temperatures were determined by differential thermal analysis (DTA) using a DTG-60A thermal analyzer. A small piece of the cold pressed pellet (5.4 mg) with $LaMgNi_4/LaNi_5$ molar ratio of 1:3 was used for the DTA test. The testing temperature was increased from 723 K to 1293 K with the heating rate of 5 K min^{-1}. High purity argon was used as the carrier gas with the flow rate of 20 ml min^{-1}. The sintering temperatures applied to prepare the single-phase La_2MgNi_9, La_3MgNi_{14} and La_4MgNi_{19} alloys in this study were ca. 50–100 K higher than the detected temperatures from the DTA result to ensure a complete reaction of the precursors. A long period of annealing was performed after sintering to ensure the homogeneity of the alloy samples. The temperatures for the subsequent annealing process were chosen to be 50–100 K lower than their corresponding peritectic reaction temperatures. The chemical compositions of the final pellets were examined by inductively coupled plasma (ICP) system.

The alloys were ground to powders below 300 mesh for X-ray diffraction (XRD) measurement. The measurement was performed with a D/Max-2500/PC X-ray diffractometer with Cu Kα1 radiation, and the XRD patterns were analyzed by Rietveld method [13] using Maud software [14]. The morphologies of the alloy samples were observed using an S-4800 scanning electron microscope (SEM) in backscattering electron (BSE) mode.

To investigate the hydrogen absorption/desorption properties of the alloy samples, pressure-composition-temperature (*P-C-T*) isotherms were measured using a Sieverts-type apparatus at 30, 50, and 70 °C. Prior to the measurement, the samples were hydrogenated/dehydrogenated for 3 cycles at 80 °C for activation.

The testing electrodes for electrochemical measurements were prepared as follows: Firstly, the alloy powder of 200–400 mesh was mixed with carbonyl Ni powder in a weight ratio of 1:5. The mixtures were then cold pressed into pellets under 15 MPa. Each of the resulting pellets was sandwiched between two Ni foams and welded to a nickel stick. Electrochemical properties of the alloy samples were tested in a three-electrode system with a 6 M KOH solution as electrolyte at room temperature. A sintered $Ni(OH)_2$ electrode was used as the counter electrode and a Hg/HgO electrode was used as the reference electrode. The test electrodes were activated at a rate of 0.2 C for seven charge/discharge cycles. Then, the rate capability and cycling stability were evaluated galvanostatically. The end potential of the discharge was set at −0.6 V vs. the